

Published in final edited form as:

Cell Metab. 2011 March 2; 13(3): 249–259. doi:10.1016/j.cmet.2011.02.005.

Transcriptional control of adipose lipid handling by IRF4

Jun Eguchi¹, Xun Wang¹, Songtao Yu², Erin E. Kershaw³, Patricia C. Chiu¹, Joanne Dushay¹, Jennifer L. Estall⁴, Ulf Klein⁵, Eleftheria Maratos-Flier¹, and Evan D. Rosen¹

¹ Division of Endocrinology, Beth Israel Deaconess Medical Center, Boston, MA 02215

² Department of Pediatrics, Children's Memorial Research Center, Northwestern University Feinberg School of Medicine, Chicago, IL 60614

³ Division of Endocrinology, University of Pittsburgh, Pittsburgh, PA 15261

⁴ Department of Cancer Biology, Dana-Farber Cancer Institute, Boston, MA 02215

⁵ Herbert Irving Comprehensive Cancer Center, Columbia University, New York City, NY 10032

Summary

Adipocytes store triglyceride during periods of nutritional affluence and release free fatty acids during fasting through coordinated cycles of lipogenesis and lipolysis. While much is known about the acute regulation of these processes during fasting and feeding, less is understood about the transcriptional basis by which adipocytes control lipid handling. Here we show that interferon regulatory factor 4 (IRF4) is a critical determinant of the transcriptional response to nutrient availability in adipocytes. Fasting induces IRF4 in an insulin- and FoxO1-dependent manner. IRF4 is required for lipolysis, at least in part due to direct effects on the expression of adipocyte triglyceride lipase and hormone-sensitive lipase. Conversely, reduction of IRF4 enhances lipid synthesis. Mice lacking adipocyte IRF4 exhibit increased adiposity and deficient lipolysis. These studies establish a link between IRF4 and the disposition of calories in adipose tissue, with consequences for systemic metabolic homeostasis.

Introduction

The current epidemic of obesity has prompted intense investigation into the molecular mechanisms underlying fat storage and utilization (Bluher, 2009; Jensen, 2008). Adipose tissue is the dominant site for storage of excess energy derived from food intake. Factors that control the synthesis of fat (lipogenesis) and fat mobilization (lipolysis) are important regulators of triacylglycerol (TAG) accumulation in adipose tissue (Bouchard et al., 1993; Lafontan, 2008). In the fed state, fatty acids (FA) are synthesized in adipocytes through *de novo* lipogenesis from non-lipid substrates, and subsequently esterified into TAG. Conversely, in the fasted state, TAG are broken down into free fatty acids (FFA) and glycerol, which are released to supply the energy needs of other tissues. FFA and glycerol are substrates for ketogenesis and gluconeogenesis, respectively, in the liver, and FFA is used by skeletal muscle and heart as an energy source (Duncan et al., 2007).

© 2011 Elsevier Inc. All rights reserved.

Corresponding Author: Evan D. Rosen, MD, Ph.D Division of Endocrinology and Metabolism Beth Israel Deaconess Medical Center 330 Brookline Ave E/CLS743 Boston, MA 02215 P: 617-735-3221 F: 617-735-3323 erosen@bidmc.harvard.edu .

Publisher's Disclaimer: This is a PDF file of an unedited manuscript that has been accepted for publication. As a service to our customers we are providing this early version of the manuscript. The manuscript will undergo copyediting, typesetting, and review of the resulting proof before it is published in its final citable form. Please note that during the production process errors may be discovered which could affect the content, and all legal disclaimers that apply to the journal pertain.

During cycles of fasting and feeding, adipose tissue lipid metabolism is controlled by nutrients (such as carbohydrates and polyunsaturated fatty acids) and by hormones (such as insulin and catecholamines); the normal interplay of these factors is essential to maintain normal adipose homeostasis. During feeding, insulin exerts its pro-lipogenic functions via a transcription factor called sterol regulatory element binding protein 1c (SREBP1c), while the effects of carbohydrates and polyunsaturated fatty acids are mediated by carbohydrate response element binding protein (ChREBP) and liver \times receptor (LXR), respectively (Darimont et al., 2006; Eberle et al., 2004; Kersten, 2001; Kim et al., 1998; Uyeda et al., 2002). In contrast, the transcriptional regulation of lipolysis is less well defined.

The recent realization that obesity represents a state of chronic inflammation has led to the identification of many genes and proteins, previously thought to act specifically on immune function, as key regulators of metabolism (Hotamisligil and Erbay, 2008). We previously identified interferon regulatory factors (IRFs) during an unbiased search for novel transcriptional regulators of adipogenesis based on DNase hypersensitivity (Eguchi et al., 2008). IRFs are a family of transcription factors involved in a wide range of immune functions, including lymphopoiesis, macrophage differentiation and the regulation of innate immunity, particularly as effectors of toll-like receptor (TLR) signaling (Honda and Taniguchi, 2006; Tamura et al., 2008). All nine mammalian IRFs are expressed in adipose tissue in a developmentally-regulated manner, and IRF1, IRF3, and IRF4 exhibit anti-adipogenic properties in cultured adipocytes (Eguchi et al., 2008). Our previous study showed that unlike other IRF members, IRF4 expression is highly restricted to immune cells and adipose tissue, and is more abundant in mature adipocytes than other cell types in adipose tissue. Additionally, IRF4 expression rises during differentiation, further suggesting a role in the mature adipocyte (Eguchi et al., 2008). IRF4 has been studied in the context of immune regulation, and has been shown to be involved in lymphoid, myeloid, and dendritic cell development (Busslinger, 2004; Lohoff et al., 2002; Taylor et al., 2006). There is no data describing a role for IRF4 in cellular or organismal metabolism.

To elucidate the functional role of IRF4 in adipocytes, we studied IRF4 deficient cells and mice lacking IRF4 specifically in adipocytes. Here we show that IRF4 expression is nutritionally regulated, an effect mediated by the actions of insulin on FoxO1. Furthermore, we demonstrate that IRF4 plays a significant role in the transcriptional regulation of lipid handling in adipocytes, with consequences for nutrient partitioning and overall adiposity.

Results

IRF4 gene expression is nutritionally regulated in adipocytes

To investigate a role for IRF4 in mature adipocytes, we began by asking whether IRF4 is nutritionally regulated. Twenty-four hours of fasting resulted in dramatic induction of IRF4 at both the mRNA (Fig. 1A) and protein (Fig. 1B) level in white adipose tissue (WAT) and brown adipose tissue (BAT), with subsequent down-regulation following refeeding. This effect is not seen in spleen, one of the few tissues other than fat that expresses significant levels of IRF4. The time course for this effect is relatively swift, with significant up-regulation of *Irf4* mRNA within 6 hours of food withdrawal, and repression within an hour of refeeding (Fig. S1A). We noted similar regulation of IRF4 in subcutaneous and epididymal WAT depots (Fig. S1B). We next sought to determine if this was a rodent-specific effect or whether it could be relevant to humans. Biopsy samples were obtained from the subcutaneous fat of male volunteers before and after 72 hours of fasting (see Table S1 for clinical characteristics). Indeed, *IRF4* mRNA rose significantly with fasting in five of seven patients (Fig. 1C; $p < 0.05$). The effect of fasting and feeding on IRF4 gene expression in adipose tissue thus appears to be a conserved response with relevance to human biology,

although because these samples were not fractionated, we cannot be certain that the effect is contained within the mature adipocyte *per se*.

Insulin regulates *Irf4* expression via effects on FoxO1

Adipose tissue is insulin-sensitive, while spleen is not; the fact that IRF4 expression is regulated in the former but not the latter suggested to us that insulin might repress IRF4. This proved to be the case, as cultured 3T3-L1 adipocytes treated with insulin showed a dose- and time-dependent reduction in *Irf4* mRNA levels (Fig. 1D and Fig. S1C). To determine whether insulin plays a similar role *in vivo*, we examined adipose tissue from mice treated with streptozotocin, which causes β -cell failure and insulinopenia. In these animals, *Irf4* mRNA expression in WAT rose significantly, and decreased when insulin was replaced (Fig. 1E). Similarly, *Irf4* mRNA levels were elevated in mice lacking insulin receptors exclusively in adipose tissue [so-called Fat specific Insulin Receptor Knockout (FIRKO) mice (Bluher et al., 2002)] (Fig. 1F). Taken together, these findings indicate that insulin is a potent repressor of IRF4 expression, and implicate the rise and fall of insulin during feeding and fasting as a dominant determinant of IRF4 levels in fat. Consistent with this notion, IRF4 expression is repressed in whole WAT of three different rodent models of obesity, a hyperinsulinemic state (Fig. S1D). As previously reported (Joken et al., 2007; Kershaw et al., 2007), there was also a significant reduction of ATGL mRNA in whole WAT of high-fat diet induced obesity and *ob/ob* mice compared to controls (Fig. S1D). Fractionation reveals that the obesity-induced reduction of *Irf4* in whole WAT predominantly reflects an effect in mature adipocytes; high-fat feeding induces an increase in stromal-vascular IRF4 content, consistent with adipose infiltration of macrophages (which also express a significant amount of IRF4) in obesity (Fig. S1E).

Many gene expression events affected by insulin are mediated by the transcription factor forkhead box O1 (FoxO1), which is phosphorylated and subsequently excluded from the nucleus upon insulin stimulation (Biggs et al., 1999; Kops et al., 1999; Nakae et al., 2000). To assess whether FoxO1 is an upstream regulator of *Irf4* transcription, we introduced wild-type FoxO1 (WT), a constitutively active mutant FoxO1 (CA), a dominant negative FoxO1 mutant (DN), or EGFP control into mature 3T3-L1 Δ CAR cells using adenovirus. Ectopic overexpression of WT and CA FoxO1 caused a significant increase in basal *Irf4* mRNA levels, while the DN mutant had the opposite effect (Fig. 1G). Although insulin stimulation could still diminish *Irf4* mRNA levels in WT cells, this effect was blocked in CA cells. *In silico* analysis identified at least four predicted FoxO1 binding sites in the proximal 8 kb of the murine *Irf4* upstream flanking sequence. We used serial deletion analysis of this region in a luciferase reporter to identify the region between 1250 and 1320 base pairs upstream of the *Irf4* transcriptional start site as the insulin-responsive locus (Fig. 1H), and chromatin immunoprecipitation (ChIP) assay in 3T3-L1 adipocytes confirmed direct, insulin-sensitive FoxO1 binding to this region (Fig. 1I).

IRF4 is required for lipolysis *in vitro*

Given the profound induction of IRF4 in fasted adipocytes, we postulated a role for this transcription factor in lipolysis. To address this, we generated immortalized lines of wild-type (WT) and *Irf4*^{-/-} (KO) mouse embryonic fibroblasts (MEFs), and then used retroviral expression of C/EBP α to convert these cells into adipocytes. Oil red O staining and adipocyte marker gene expression demonstrated that equal degrees of differentiation were achieved in both cell lines (Fig. S2A and S2B). As predicted, isoproterenol-stimulated lipolysis was diminished in adipocytes lacking IRF4 (Fig. 2A). The converse was also true; forced IRF4 overexpression in mature WT and KO adipocytes enhanced lipolysis in the presence of isoproterenol (Fig. 2A). IRF4 is a transcription factor, so we hypothesized that expression of key lipases might be affected by its absence. Indeed, loss of IRF4

corresponded to a significant reduction in the mRNA (Fig. 2B) and protein levels (Fig. 2C) of *Lipe* (encoding HSL) and *Pnpla2* (encoding ATGL). As in MEFs, forced IRF4 overexpression (Fig. S2C) in mature 3T3-L1 adipocytes significantly enhanced lipolysis in the presence of isoproterenol (Fig. S2D) and increased the expression of *Lipe* and *Pnpla2* mRNA (Fig. S2E).

To investigate possible direct regulation of lipase gene expression by IRF4, we performed transactivation assays in 3T3-L1 cells. These studies demonstrated that IRF4 induced reporter expression through predicted ISRE binding sites in the upstream flanking region of *Pnpla2* (Fig. 2D), and ChIP assay confirmed IRF4 binding to one of these sites (Fig. 2E). While binding was detected at several putative ISRE sites in the *Lipe* promoter, IRF4 was able to induce reporter expression even in the absence of these motifs, suggesting the existence of an additional cryptic binding site in the proximal promoter (Fig. S2F and S2G). These data indicate that IRF4 is required for lipolysis, at least in part through direct induction of ATGL and HSL.

IRF4 inhibits lipogenesis

During feeding, adipose tissue stores excess calories as triglyceride. While some lipids are imported directly from the circulation, adipocytes also perform *de novo* lipogenesis. Because lipolysis and lipogenesis are functionally opposed, we speculated that IRF4 might act to suppress lipogenesis and triglyceride synthesis. This proved to be the case, as insulin was able to increase the rate of lipid synthesis in KO adipocytes to a greater degree than in WT cells (Fig. 3A). Furthermore, forced expression of IRF4 suppressed insulin-stimulated lipid synthesis, and was able to fully revert the lipogenic phenotype of cells lacking *Irf4*.

Consistent with the effect on lipogenesis, the expression of genes related to lipid synthesis was regulated by IRF4 (Fig. 3B). All lipid synthesis genes tested were repressed at least somewhat by exogenous IRF4, whereas ablation of IRF4 led to significant increases in select targets only, such as *Scd1*, *Fasn*, *Srebfl*, and *Me1*. Taken together, our data demonstrates coordinated regulation of lipid synthesis and breakdown in cultured adipocytes.

Fat-specific deletion of IRF4 results in increased adiposity

We sought next to extend our *in vitro* findings to a more physiologically relevant system. Because we wished to avoid confounding effects in macrophages or other immune cell types, we focused on a model that would allow observation of adipocyte-specific actions of IRF4 *in vivo*. To that end, we generated a BAC transgenic mouse in which Cre recombinase was inserted into the starting ATG of *Adipoq*, which encodes adiponectin (See Methods). These mice express Cre recombinase in a highly adipocyte-specific manner, with no expression in stimulated or resident macrophages (Fig. S3A-D). We crossed these Adipoq-Cre mice to *Irf4^{fllox/+}* mice to allow generation of fat-specific IRF4 knockout mice (hereafter referred to as FI4KO). FI4KO mice showed virtually complete absence of IRF4 mRNA and protein specifically in WAT and BAT, with intact IRF4 expression in spleen and macrophages (Figs. 4A and 4B). In addition to confirming the absence of IRF4, we also examined expression of the eight other IRF family members for possible compensatory regulation. As we reported previously, all IRF family members are detectable in WAT. We noted that IRF6, IRF7, and IRF9 were up-regulated in the absence of IRF4, however, the significance of this up-regulation is uncertain; IRF6 and IRF9 in particular are expressed at much lower absolute levels than IRF4 (Fig. S4E). FI4KO mice were born in a Mendelian ratio, and there were no obvious morphological differences from control mice (WT, Adipoq-Cre only, or Flox) in young animals (data not shown). On chow diet, total body weight was not different from controls, although MRI revealed a small but significant excess of adipose

mass in 18-week old FI4KO animals (Fig. S4A and S4B). Histological analysis and cell size measurement of WAT showed slightly larger adipocytes in FI4KO mice than in littermate controls (Fig. S4C and S4D). When placed on a high-fat diet, the body weight of FI4KO mice was significantly greater than that of littermates (Figs. 4C and 4E), with the difference explained entirely by excess adiposity and larger fat cells (Figs. 4D, 4F, and 4G). Interscapular brown adipose tissue (BAT) mass was also enlarged in high-fat fed FI4KO mice (Figs. 4H). There was no obvious difference in hepatic lipid content between Flox and FI4KO animals (data not shown). FI4KO mice on high-fat diet showed impaired glucose and insulin tolerance to a degree consistent with their increased body weight (Fig. S5A,B). We were unable to detect a difference in food intake or locomotor activity; FI4KO mice showed somewhat reduced oxygen consumption and CO₂ production when normalized by body weight (Fig. S6A-C). This difference disappeared, however, when normalized on a per animal basis.

FI4KO mice exhibit diminished lipolysis

Based on the *in vitro* lipolysis data and the excess adiposity seen in FI4KO mice, we speculated that IRF4 may be required for normal lipolysis *in vivo*. To directly test this hypothesis, we measured serum glycerol and non-esterified fatty acids (NEFA) under basal and isoproterenol-stimulated conditions. Consistent with the *in vitro* data, FI4KO mice displayed reduced isoproterenol-stimulated lipolysis (Fig. 5A). We also tested this after high-fat feeding and saw the same result for NEFA, but not glycerol (Fig. S7). To determine if this effect was truly cell autonomous, we isolated primary adipocytes from *Irf4^{flox/flox}* and FI4KO mice, and compared lipolysis in these cells in the *ex vivo* setting. Indeed, primary adipocytes from FI4KO mice display reduced lipolysis in both the basal and catecholamine-stimulated state (Fig. 5B and 5C). Q-PCR analysis demonstrated reduced fasting *Pnpla2* and *Lipe* expression (Fig. 5D). Conversely, and consistent with the *in vitro* data, genes of lipid uptake (e.g. *Slc27a1* and *Cd36*) and lipid synthesis (e.g. *Dgat1*, *Dgat2*, and *Fasn*) show enhanced expression in the fed state in FI4KO mice (Fig. 5D). These data suggest that reduced lipolysis and increased lipogenesis in fat may be reflected in the higher adiposity of FI4KO mice.

Finally, we sought to test the ability of FI4KO mice to respond to two situations that require lipolysis. First, we subjected FI4KO and control mice to a prolonged fast of 48 hours. FI4KO mice lost less body fat than control mice during this provocation (Fig. 6A), consistent with their lower serum non-esterified fatty acids and β -hydroxybutyrate (Fig. 6B).

We next examined cold-induced thermogenesis of Flox and FI4KO mice. At an ambient temperature of 22°C, Flox and FI4KO mice had similar body temperatures. However, at 4°C, FI4KO mice experienced a much more rapid decline in body temperature than seen in Flox mice (Fig. 7A). Furthermore, cold exposure was much less able to induce *Ucp1* and *Pgc1 α* in BAT of FI4KO mice (Fig. 7B).

DISCUSSION

IRF4 is a well-known participant in a variety of immune activities, including regulatory T cell function and the development of inflammatory T(H)-17 cells, as well as plasma cell differentiation (Brustle et al., 2007; Klein et al., 2006; Mittrucker et al., 1997; Zheng et al., 2009). Mice made globally deficient in IRF4 develop lymphadenopathy and lack functional germinal B cell centers and normal plasma cells (Mittrucker et al., 1997). Previously, we identified WAT and BAT as major sites of IRF4 expression, though its function in these tissues was not apparent. The discovery that IRF4 expression is extraordinarily sensitive to fasting and feeding suggested a role in nutrient partitioning.

Metabolic control of lipolysis has been most intensively studied at the level of nutritionally-sensitive signal transduction cascades, rather than transcriptional regulation. Lipolysis is induced acutely in fasting by β -adrenergic signaling leading to cAMP accumulation and subsequent PKA-mediated phosphorylation of HSL and the lipid droplet protein perilipin (Carmen and Victor, 2006; Jocken and Blaak, 2008). In the fed state, insulin inhibits lipolysis via mechanisms that are somewhat less clear, although a role has been postulated for insulin-mediated activation of phosphodiesterase 3B, which hydrolyzes cAMP (Kitamura et al., 1999; Wijkander et al., 1998). Our work demonstrates an additional mechanism by which insulin inhibits lipolysis, albeit on a longer time scale, through the cytosolic sequestration of FoxO1 and subsequent reduction of IRF4 expression. IRF4 promotes lipolysis, at least in part, by inducing the expression of the lipases ATGL and HSL. These data are consistent with prior studies showing that insulin regulates ATGL expression in 3T3-L1 cells and mice (Kershaw et al., 2006). Interestingly, FoxO1 has been shown to directly activate the *Pnpla2* promoter in 3T3-L1 adipocytes (Chakrabarti and Kandror, 2009). Our discovery that FoxO1 directly induces IRF4 implies the existence of an insulin-repressible feed-forward loop involving these two factors. Several other factors have recently been discovered to acutely regulate lipolysis, such as CGI-58 (Lass et al., 2006), AdPLA (Jaworski et al., 2009), and G0S2 (Yang et al., 2010), however we have not been able to demonstrate significant effects of IRF4 on the expression of any of these mediators (not shown). Similarly, we have looked at upstream components of the lipolysis machinery, including levels of cAMP and phospho-HSL, but have so far not found significant or consistent IRF4-dependent effects (not shown).

Lipogenesis is regulated by the nutritional environment, in particular by feeding and fasting. In adipocytes, lipogenesis is activated by a high carbohydrate supply and by the actions of insulin. These actions are mediated by transcription factors such as SREBP1c, ChREBP, and LXR. We have shown that IRF4 inhibits insulin-induced lipogenesis in cultured adipocytes, and that IRF4 is associated with reduced expression of genes related to lipid synthesis. It is not yet clear, however, which genes are most relevant to the repression of lipogenesis by IRF4, or whether the effect is direct or indirect. It is worth noting that the effect of IRF4 on lipogenic gene expression was only seen in the fed state, which is when insulin levels are highest. This may seem counterintuitive, given our demonstration that insulin represses IRF4 expression. However, IRF4 expression is still detectable after feeding, and this appears to be sufficient to repress lipogenic genes.

While we focused on the actions of IRF4 in WAT, our data supports an effect in BAT as well. FI4KO mice (which express Cre in BAT as well as WAT) showed increased BAT mass associated with larger lipid droplets. Furthermore, FI4KO mice were cold-intolerant. This phenomenon may be due to reduced fatty acid availability from WAT stores preventing optimal BAT function by diminishing substrate. However, we also see reduced PGC-1 α and UCP-1 expression in the BAT of FI4KO mice, suggesting additional mechanisms may be at play, such as abnormal adrenergic signaling.

Interestingly, *Irf4* mRNA levels are reduced in obesity. This may seem paradoxical given that obesity is associated with insulin resistance, and mice lacking insulin receptors in fat display elevated *Irf4* expression. However, the insulin resistance associated with obesity is defined by its effects on the metabolic actions of insulin. Many genes respond normally to insulin even in the context of 'insulin resistance' (Samad et al., 2000; Sartipy and Loskutoff, 2003). It also remains possible that other factors dominate the control of *Irf4* gene expression in the context of obesity.

While IRF4 is believed to act primarily as a transcription factor, there are some data from macrophages suggesting that it may appear in the cytosol in small amounts where it can bind

and inhibit TLR4 (Honma et al., 2005; Negishi et al., 2005). TLR4 signaling, however, is known to *activate* lipolysis (Zu et al., 2009), making this an unlikely mechanism for the pro-lipolytic actions of IRF4. Definitive proof of this will require experiments using DNA binding mutant alleles of IRF4.

Because IRF4 is expressed in macrophages and lymphocytes, both of which can affect metabolic pathways in adipose tissue (Honma et al., 2005; Marecki et al., 1999; Tamura et al., 2008), we sought to perform studies *in vivo* using a model that would reduce or eliminate confounding effects from immune cell types. Cre-lox recombination offers such an opportunity, however, the traditional adipose-selective Cre-driver mouse uses the *Fabp4* (also called aP2) promoter (Abel et al., 2001; Barlow et al., 1997). This is problematic because *Fabp4* is expressed in macrophages as well as fat (Fu et al., 2002; Makowski et al., 2001). Additionally, other problems have been associated with the *Fabp4*-Cre mouse, including poor recombination efficiency (Halberg et al., 2009). To circumvent these issues, we generated an adipose-specific Cre BAC transgenic mouse line, in which Cre recombinase was inserted into the starting ATG of the adiponectin (*Adipoq*) locus. These mice express Cre effectively in WAT and BAT but not in macrophages, including adipose-tissue resident macrophages, alveolar macrophages, or thioglycollate-stimulated peritoneal macrophages. These mice, which we call *Adipoq*-Cre, thus provide a new and highly effective reagent for adipose-specific gene loxP-mediated gene recombination. We note that another group has recently generated their own version of these mice, using a 5.4 kb promoter fragment of the *Adipoq* gene rather than an intact BAC (Wang et al.).

FI4KO mice display increased adiposity, and are resistant to lipolysis induced by catecholamines, fasting, or cold exposure. Depletion of IRF4 in WAT also impaired the normal regulation of lipid synthesis genes (*Plin2*, *Fasn*, *Slc27a1*, and *CD36*) during the fasting and feeding cycle. Taken together with our *in vitro* observations, IRF4 appears to be a critical transcriptional regulator of lipid handling in fat. There is significant interest in developing anti-inflammatory drugs as therapy for metabolic diseases like Type 2 diabetes. Some ‘inflammatory’ proteins however, like IRF4, may play key roles in metabolic function independent of their effect on immunity. Such nuances will need to be fully explored before the potential of this therapeutic avenue can be fully realized.

Experimental Procedures

Materials

Antibodies for Western blotting were purchased from Santa Cruz Biotechnology (IRF4, sc-6059; Actin, sc-1615), Cell Signaling Technology (ATGL, 2138; HSL, 4107) and Millipore, Inc. (Tubulin, MAB3408). The coding region of mouse IRF4 was isolated from 3T3-L1 adipocyte mRNA by RT-PCR using TaKaRa EX Taq polymerase (Takara Bio Inc.) and subcloned into pCDH-puro lentiviral vector (System Biosciences) for expression in mammalian cells. The coding sequence of mouse C/EBP α was subcloned into pREV-TRE-hygro retroviral vector as described (Zuo et al., 2006). Adenoviral vectors for EGFP, FoxO1, ADA (constitutive active mutant), and Δ 256 (dominant negative mutant) were made in pAxCawt (Takara Bio Inc.) as described (Nakae et al., 2001). All FoxO1 constructs were the generous gift of Dr. D. Acilli.

Cell culture

3T3-L1 cells (American Type Culture Collection) or 3T3-L1 Δ CAR cells (Orlicky et al., 2001) were cultured in Dulbecco’s modified Eagle’s medium (DMEM) (Invitrogen) with 10% Bovine Calf Serum (BCS; Hyclone) in 5% CO₂. Two days post confluence, cells were exposed to DMEM/10% Fetal Bovine Serum (FBS; Invitrogen) with 1 μ M dexamethasone

(Sigma), 5 μ g/ml insulin (Sigma), and 0.5mM isobutylmethylxanthine (Sigma). After 2 days, cells were maintained in medium containing FBS only. For insulin regulation experiments, fully differentiated 3T3-L1 adipocytes were incubated in serum-free DMEM containing 1% fatty acid-free BSA (Sigma) with and without bovine insulin at the doses and times indicated.

Generation and differentiation of immortalized mouse embryonic fibroblasts (MEFs)

Irf4^{+/-} mice were generated as previously described (Mittrucker et al., 1997). Male and female *Irf4*^{+/-} mice were mated, and embryos were harvested at e12.5. Primary MEFs were generated and plated as monolayer cultures in DMEM with 10% FBS as described previously (Rosen et al., 2002). Primary MEFs were immortalized by plating 3 \times 10⁵ cells per 60-mm dish every 3 days as described (Todaro and Green, 1963). The C/EBP α -pMSCV construct was transfected into Phoenix packaging cells using the CellPfect transfection kit (Amersham Biosciences). Immortalized MEFs were transduced with viral supernatants and selected in hygromycin. Two days post confluence, cells were exposed to DMEM/10% FBS with dexamethasone (1 μ M), insulin (5 μ g/ml), isobutylmethylxanthine (0.5mM), and rosiglitazone (1 μ M). After 2 days, cells were maintained in medium containing FBS only.

Animals

Fasting and feeding studies were performed using FVB mice obtained from Charles River Laboratories and fed a standard diet (8664, Harlan Teklad). Mice were maintained under a 14 hr light/10 hr dark cycle at constant temperature (22°C) with free access to food and water. To determine the effect of nutritional status, 10-week-old male FVB mice were fed *ad libitum*, fasted for 24h, or re-fed for 24h after the 24-h fast (n=7-8). To determine the effect of insulin deficiency and replacement on IRF4 mRNA expression, 10-week old male C57BL/6J mice were treated with streptozotocin (STZ) with or without insulin replacement as described (Kershaw et al., 2006). All animal studies were approved by the Institutional Animal Care and Use Committee of Beth Israel Deaconess Medical Center. White adipose tissue (WAT) of Fat-specific insulin receptor knockout (FIRKO) mice were generously provided by Dr. C. Ronald Kahn. The 16-week-old *ob/ob* and *db/db* mice were purchased from the Jackson Laboratory. For DIO mice, C57BL/6J mice were fed a high-fat diet (D12331; Research Diets Inc.) for 12 weeks. Body weight and food intake were measured weekly. Mice were subjected to Magnetic Resonance Imaging (MRI) (Echo Medical Systems) to examine body composition.

Generation of Adipoq-Cre transgenic mice

A C57Bl/6 mouse bacterial artificial chromosome (90G21) containing the *Adipoq* gene was transformed into the recombinogenic EL250 bacteria cells, and homologous recombination was performed as described elsewhere (Lee et al., 2001). The Cre-FRT-Kan-FRT cassette was transformed into the Adipoq BAC host EL250 cells and recombined to insert the Cre ATG into the *Adipoq* ATG with a resulting deletion of 222 bp of the *Adipoq* gene. Adipoq-Cre-FRT-Kan-FRT BAC host EL250 clones were identified by PCR screening. The FRT-Kan-FRT cassette was removed and an Adipoq-Cre BAC host EL250 clone without mutation in the Cre coding sequence was obtained. The loxP site present in the vector sequence of the Adipoq-Cre BAC was removed. The transgenic construct was microinjected into pronuclei of fertilized one-cell stage embryos of FVB mice (Jackson Laboratories) using standard methods. Twelve founders were obtained. The Adipoq-Cre founder was backcrossed >8 times onto C57BL/6J prior to use in these experiments. Adipoq-Cre mice have been deposited at the Jackson Laboratory Repository with JAX Stock No. 010803.

Generation of FI4KO mice

Irf4^{flox/flox} mice were generated as described previously (Klein et al., 2006). Adipoq-Cre mice were mated with *Irf4^{flox/flox}* mice, and cohorts were established by mating F1 *Irf4^{flox/+}; Cre⁺* mice to littermate *Irf4^{flox/+}; Cre⁻* mice. Mice were maintained under a 14 hr light/10 hr dark cycle at constant temperature (22°C) with free access to food and water and were fed either a standard chow diet (8664, Harlan Teklad) or a high fat diet (D12331; Research Diets Inc.).

Isolation of primary cells

Adipocytes were isolated from epididymal fat depots in Krebs-Ringer HEPES (KRH) buffer by collagenase digestion as described (Joost and Schurmann, 2001). Peritoneal macrophages from Adipoq-Cre, *Irf4^{flox/flox}* mice and FI4KO mice were isolated by peritoneal lavage 4 days after injection of 3% thioglycollate (2.5ml i.p. ; Difco; BD Diagnostics).

Measurement of adipocyte size

Epididymal WAT were isolated and fixed in osmium tetroxide solution (Sigma-Aldrich). The distribution of adipocyte size in WAT were analyzed by a Coulter counter (Multisizer II, Coulter Electronics) as described previously (DiGirolamo and Fine, 2001).

Serum analysis

After collection of serum from tail vein, β -hydroxybutyrate (StanBio) and nonesterified fatty acids (NEFAs) (Wako Chemicals) were measured in duplicate using colorimetric assays.

Cold-induced thermogenesis

Rectal temperature was measured using a rectal probe (Yellow Spring Instruments Co.) in Flox and FI4KO (KO) mice under the cold exposure.

Indirect Calorimetry

Metabolic rate of mice was measured by indirect calorimetry in open-circuit oxymax chambers that are a component of the Comprehensive Lab Animal Monitoring System (CLAMS; Columbus Instruments, Columbus, OH). Mice were housed individually and maintained at 22°C under a 12:12-h light-dark cycle. Food and water were available ad libitum.

Human subjects

Healthy male adults ages 18-60, BMI 19-39 kg/m² without significant medical illness were recruited by advertisement for participation. Individuals with diabetes, heart disease, liver disease, renal insufficiency, thyroid disease, gout or a history of kidney stones were excluded. Individuals with a history of alcohol abuse or marijuana use were also excluded. Subjects reported stable weight (+/- 3kg) for 6 months prior to participation. All subjects underwent a screening visit that included a medical history, physical exam and baseline laboratory tests. Patients gave written informed consent to all clinical investigations, which were performed in accordance with the principles embodied in the Declaration of Helsinki. The protocols were conducted in accordance with the ethical standards of the Committee on Clinical Investigation and were approved by the Beth Israel Deaconess Medical Center Institutional Review Board. The studies were conducted from June, 2007 to April, 2010 at the Beth Israel Deaconess Medical Center, General Clinical Research Center, Boston, MA ClinicalTrials.gov identifier: NCT00476125. Following a screening visit, 5 healthy, lean male subjects reported to the GCRC at 8am for a standard 500 calorie breakfast. One hour after the meal, subjects underwent a subcutaneous fat biopsy and then began fasting.

Subjects were typically fasted for 72 hours, except one individual who terminated the fast after 50 hours due to fatigue. Body weight and body composition were measured daily. A second subcutaneous fat biopsy was done at the end of the fasting period, before the subject was fed a standard meal. Clinical data are presented in Supplemental Table 1.

Analysis of Gene Expression by Q-PCR

Total RNA was extracted from cells or tissues using TRIzol reagent (Invitrogen) following the manufacturer's instructions. First-strand cDNA synthesis was performed using RETROscript (Ambion). Total RNA was converted into first-strand cDNA using oligo(dT) primers as described by the manufacturer. PCR was performed using cDNA synthesized from 1.5 µg total RNA in an Mx3000P Q-PCR system (Stratagene) with specific primers and SYBR Green PCR Master Mix (Stratagene). The relative abundance of mRNAs was standardized using *36B4* mRNA as the invariant control. Primers used are listed in Supplemental Table 2.

Luciferase Reporter Assay

The indicated regions of the murine *Irf4*, *Pnpla2* (ATGL), and *Lipe* (HSL) promoters were PCR amplified and ligated into pGL3-Basic (Promega). Five days after adipogenic stimulation, 3T3-L1 adipocytes were detached with trypsin and transfected using the Amaxa nucleofection system (Amaxa Biosystems). Transfections were performed using 2 µg of reporter construct along with 100ng of IRF4-pCDH expression vector or EGFP-pCDH, with 100ng of galactosidase expression vector as a transfection control. Luciferase activity was measured 24 hr after transfection using the Galacto-Star luciferase reporter assay (Roche) according to the manufacturer's instructions.

Chromatin Immunoprecipitation

3T3-L1 cells were treated with 1% formaldehyde for 10 min at room temperature to crosslink DNA-protein complexes. Genomic DNA was sheared using a Sonic Dismembrator Model 100 (Fisher Scientific) to obtain fragments ranging from 200 bp to 1 kb. ChIP was performed using a kit from Upstate, with 3 µg of primary antibody, goat IgG, or rabbit IgG. The following primary antibodies were used: goat anti-IRF4 (sc-6059), or rabbit anti-FoxO1 (sc-11350) (Santa Cruz Biotechnology). Crosslinking was reversed and purified DNA was subjected to Q-PCR using SYBR green fluorescent dye (Stratagene). Primers used are listed in Supplemental Table 2.

Protein Extraction and Western Blot Analysis

Tissue and cell lysates were prepared using RIPA buffer (Boston BioProducts) supplemented with complete protease inhibitor cocktail (Roche). For Western blot analyses, 50 µg of protein was subjected to SDS-PAGE under reducing conditions, transferred, and blotted using the anti-IRF4 antibody described above.

Lipolysis assay

For *in vitro* studies, adipocytes were washed twice with DMEM and then incubated for 6 h in serum-free DMEM containing 1% fatty acid-free BSA in the presence or absence of 10µM isoproterenol. Conditioned medium was then analyzed for glycerol using the Free Glycerol Determination Kit (Sigma). Adipocytes were then rinsed with PBS and harvested in RIPA buffer. The protein content of cell lysates was determined using the DC Protein Assay kit (BioRad). For *ex vivo* studies, adipocytes were isolated from epididymal fat pads by collagenase digestion. Cells were resuspended in Krebs-Ringer HEPES (KRH) buffer at 2×10^5 cells/ml. Cells were incubated in the presence or absence of 1µM isoproterenol for 0-2h at 37°C with gentle shaking. Glycerol and NEFA content of conditioned medium was

determined as above. For *in vivo* studies, mice were fasted for 4h and injected with isoproterenol (10 mg/kg body weight). Blood was collected from the tail vein before and 15 min after injection, and glycerol and NEFA content of serum was measured as above.

Lipogenesis assay

Lipogenesis assays were performed as previously described (Wiese et al., 1995). Briefly, after serum starvation, cells were incubated in the presence or absence of 10nM insulin for 15 min, and incubated with 5mM [¹⁴C]-glucose for 1h at 37°C. Cells were then washed three times with ice-cold PBS. Radiolabeled glucose incorporation into lipid was assessed by scraping cells into 1 ml PBS and shaking vigorously with 5ml of Betaflour Liquid Scintillation Fluid (National Diagnostics). After samples settled overnight, radioactivity partitioning into the organic phase was determined by scintillation counting. The protein content of cell lysates was determined using the DC Protein Assay kit.

Statistical analysis

Unpaired two-tailed Student's t tests and one-way ANOVA were used. $p < 0.05$ was considered statistically significant.

Supplementary Material

Refer to Web version on PubMed Central for supplementary material.

Acknowledgments

The authors wish to thank Dr. C.R. Kahn for use of samples from FIRKO mice, Dr. Tak Mak for *Irf4*^{-/-} mice, Drs. Shingo Kajimura, Tetsuya Hosooka, Choel Son, Junji Kawashima, Linh Vong, and Mark Herman for technical advice, Dr. Domenico Accili for FoxO1 adenoviral constructs, and members of the Rosen lab for helpful discussion. We thank Drs. Leo Otterbein and Eva Csizmadia for help with alveolar lavage and immunohistochemistry. This work was funded by the Kanae Foundation for the Promotion of Medical Science, American Heart Association Award AHA0825928D (to J.E.), and NIH R01 DK63906 and NIH R01 DK085171 (to E.D.R.).

References

- Abel ED, Peroni O, Kim JK, Kim YB, Boss O, Hadro E, Minnemann T, Shulman GI, Kahn BB. Adipose-selective targeting of the GLUT4 gene impairs insulin action in muscle and liver. *Nature*. 2001; 409:729–733. [PubMed: 11217863]
- Barlow C, Schroeder M, Lekstrom-Himes J, Kylefjord H, Deng CX, Wynshaw-Boris A, Spiegelman BM, Xanthopoulos KG. Targeted expression of Cre recombinase to adipose tissue of transgenic mice directs adipose-specific excision of loxP-flanked gene segments. *Nucleic Acids Res*. 1997; 25:2543–2545. [PubMed: 9171115]
- Biggs WH 3rd, Meisenhelder J, Hunter T, Cavenee WK, Arden KC. Protein kinase B/Akt-mediated phosphorylation promotes nuclear exclusion of the winged helix transcription factor FKHR1. *Proc Natl Acad Sci U S A*. 1999; 96:7421–7426. [PubMed: 10377430]
- Blüher M. Adipose tissue dysfunction in obesity. *Exp Clin Endocrinol Diabetes*. 2009; 117:241–250. [PubMed: 19358089]
- Blüher M, Michael MD, Peroni OD, Ueki K, Carter N, Kahn BB, Kahn CR. Adipose tissue selective insulin receptor knockout protects against obesity and obesity-related glucose intolerance. *Dev Cell*. 2002; 3:25–38. [PubMed: 12110165]
- Bouchard C, Despres JP, Mauriege P. Genetic and nongenetic determinants of regional fat distribution. *Endocr Rev*. 1993; 14:72–93. [PubMed: 8491156]
- Brustle A, Heink S, Huber M, Rosenplanter C, Stadelmann C, Yu P, Arpaia E, Mak TW, Kamradt T, Lohoff M. The development of inflammatory T(H)-17 cells requires interferon-regulatory factor 4. *Nat Immunol*. 2007; 8:958–966. [PubMed: 17676043]

- Busslinger M. Transcriptional control of early B cell development. *Annu Rev Immunol.* 2004; 22:55–79. [PubMed: 15032574]
- Carmen GY, Victor SM. Signalling mechanisms regulating lipolysis. *Cell Signal.* 2006; 18:401–408. [PubMed: 16182514]
- Chakrabarti P, Kandror KV. FoxO1 controls insulin-dependent adipose triglyceride lipase (ATGL) expression and lipolysis in adipocytes. *J Biol Chem.* 2009; 284:13296–13300. [PubMed: 19297333]
- Darimont C, Avanti O, Zbinden I, Leone-Vautravers P, Mansourian R, Giusti V, Mace K. Liver X receptor preferentially activates de novo lipogenesis in human preadipocytes. *Biochimie.* 2006; 88:309–318. [PubMed: 16298468]
- DiGirolamo M, Fine JB. Cellularity measurements. *Methods Mol Biol.* 2001; 155:65–75. [PubMed: 11293084]
- Duncan RE, Ahmadian M, Jaworski K, Sarkadi-Nagy E, Sul HS. Regulation of lipolysis in adipocytes. *Annu Rev Nutr.* 2007; 27:79–101. [PubMed: 17313320]
- Eberle D, Hegarty B, Bossard P, Ferre P, Foulfelle F. SREBP transcription factors: master regulators of lipid homeostasis. *Biochimie.* 2004; 86:839–848. [PubMed: 15589694]
- Eguchi J, Yan QW, Schones DE, Kamal M, Hsu CH, Zhang MQ, Crawford GE, Rosen ED. Interferon regulatory factors are transcriptional regulators of adipogenesis. *Cell Metab.* 2008; 7:86–94. [PubMed: 18177728]
- Fu Y, Luo N, Lopes-Virella MF, Garvey WT. The adipocyte lipid binding protein (ALBP/aP2) gene facilitates foam cell formation in human THP-1 macrophages. *Atherosclerosis.* 2002; 165:259–269. [PubMed: 12417276]
- Halberg N, Khan T, Trujillo ME, Wernstedt-Asterholm I, Attie AD, Sherwani S, Wang ZV, Landskroner-Eiger S, Dineen S, Magalang UJ, Brekken RA, Scherer PE. Hypoxia-inducible factor 1alpha induces fibrosis and insulin resistance in white adipose tissue. *Mol Cell Biol.* 2009; 29:4467–4483. [PubMed: 19546236]
- Honda K, Taniguchi T. Toll-like receptor signaling and IRF transcription factors. *IUBMB Life.* 2006; 58:290–295. [PubMed: 16754320]
- Honma K, Udono H, Kohno T, Yamamoto K, Ogawa A, Takemori T, Kumatori A, Suzuki S, Matsuyama T, Yui K. Interferon regulatory factor 4 negatively regulates the production of proinflammatory cytokines by macrophages in response to LPS. *Proc Natl Acad Sci U S A.* 2005; 102:16001–16006. [PubMed: 16243976]
- Hotamisligil GS, Erbay E. Nutrient sensing and inflammation in metabolic diseases. *Nat Rev Immunol.* 2008; 8:923–934. [PubMed: 19029988]
- Jaworski K, Ahmadian M, Duncan RE, Sarkadi-Nagy E, Varady KA, Hellerstein MK, Lee HY, Samuel VT, Shulman GI, Kim KH, de Val S, Kang C, Sul HS. AdPLA ablation increases lipolysis and prevents obesity induced by high-fat feeding or leptin deficiency. *Nat Med.* 2009; 15:159–168. [PubMed: 19136964]
- Jensen MD. Role of body fat distribution and the metabolic complications of obesity. *J Clin Endocrinol Metab.* 2008; 93:S57–63. [PubMed: 18987271]
- Jocken JW, Blaak EE. Catecholamine-induced lipolysis in adipose tissue and skeletal muscle in obesity. *Physiol Behav.* 2008; 94:219–230. [PubMed: 18262211]
- Joken JW, Langin D, Smit E, Saris WH, Valle C, Hul GB, Holm C, Arner P, Blaak EE. Adipose triglyceride lipase and hormone-sensitive lipase protein expression is decreased in the obese insulin-resistant state. *J Clin Endocrinol Metab.* 2007; 92:2292–2299. [PubMed: 17356053]
- Joost HG, Schurmann A. Subcellular fractionation of adipocytes and 3T3-L1 cells. *Methods Mol Biol.* 2001; 155:77–82. [PubMed: 11293085]
- Kershaw EE, Hamm JK, Verhagen LA, Peroni O, Katic M, Flier JS. Adipose triglyceride lipase: function, regulation by insulin, and comparison with adiponutrin. *Diabetes.* 2006; 55:148–157. [PubMed: 16380488]
- Kershaw EE, Schupp M, Guan HP, Gardner NP, Lazar MA, Flier JS. PPARgamma regulates adipose triglyceride lipase in adipocytes in vitro and in vivo. *Am J Physiol Endocrinol Metab.* 2007; 293:E1736–1745. [PubMed: 17848638]

- Kersten S. Mechanisms of nutritional and hormonal regulation of lipogenesis. *EMBO Rep.* 2001; 2:282–286. [PubMed: 11306547]
- Kim JB, Sarraf P, Wright M, Yao KM, Mueller E, Solanes G, Lowell BB, Spiegelman BM. Nutritional and insulin regulation of fatty acid synthetase and leptin gene expression through ADD1/SREBP1. *J Clin Invest.* 1998; 101:1–9. [PubMed: 9421459]
- Kitamura T, Kitamura Y, Kuroda S, Hino Y, Ando M, Kotani K, Konishi H, Matsuzaki H, Kikkawa U, Ogawa W, Kasuga M. Insulin-induced phosphorylation and activation of cyclic nucleotide phosphodiesterase 3B by the serine-threonine kinase Akt. *Mol Cell Biol.* 1999; 19:6286–6296. [PubMed: 10454575]
- Klein U, Casola S, Cattoretti G, Shen Q, Lia M, Mo T, Ludwig T, Rajewsky K, Dalla-Favera R. Transcription factor IRF4 controls plasma cell differentiation and class-switch recombination. *Nat Immunol.* 2006; 7:773–782. [PubMed: 16767092]
- Kops GJ, de Ruiter ND, De Vries-Smits AM, Powell DR, Bos JL, Burgering BM. Direct control of the Forkhead transcription factor AFX by protein kinase B. *Nature.* 1999; 398:630–634. [PubMed: 10217147]
- Lafontan M. Advances in adipose tissue metabolism. *Int J Obes (Lond).* 2008; 32(Suppl 7):S39–51. [PubMed: 19136990]
- Lass A, Zimmermann R, Haemmerle G, Riederer M, Schoiswohl G, Schweiger M, Kienesberger P, Strauss JG, Gorkiewicz G, Zechner R. Adipose triglyceride lipase-mediated lipolysis of cellular fat stores is activated by CGI-58 and defective in Chanarin-Dorfman Syndrome. *Cell Metab.* 2006; 3:309–319. [PubMed: 16679289]
- Lee EC, Yu D, de Velasco J, Martinez, Tessarollo L, Swing DA, Court DL, Jenkins NA, Copeland NG. A highly efficient Escherichia coli-based chromosome engineering system adapted for recombinogenic targeting and subcloning of BAC DNA. *Genomics.* 2001; 73:56–65. [PubMed: 11352566]
- Lohoff M, Mittrucker HW, Prechtel S, Bischof S, Sommer F, Kock S, Ferrick DA, Duncan GS, Gessner A, Mak TW. Dysregulated T helper cell differentiation in the absence of interferon regulatory factor 4. *Proc Natl Acad Sci U S A.* 2002; 99:11808–11812. [PubMed: 12189207]
- Makowski L, Boord JB, Maeda K, Babaev VR, Uysal KT, Morgan MA, Parker RA, Suttles J, Fazio S, Hotamisligil GS, Linton MF. Lack of macrophage fatty-acid-binding protein aP2 protects mice deficient in apolipoprotein E against atherosclerosis. *Nat Med.* 2001; 7:699–705. [PubMed: 11385507]
- Marecki S, Atchison ML, Fenton MJ. Differential expression and distinct functions of IFN regulatory factor 4 and IFN consensus sequence binding protein in macrophages. *J Immunol.* 1999; 163:2713–2722. [PubMed: 10453013]
- Mittrucker HW, Matsuyama T, Grossman A, Kundig TM, Potter J, Shahinian A, Wakeham A, Patterson B, Ohashi PS, Mak TW. Requirement for the transcription factor LSIRF/IRF4 for mature B and T lymphocyte function. *Science.* 1997; 275:540–543. [PubMed: 8999800]
- Nakae J, Barr V, Accili D. Differential regulation of gene expression by insulin and IGF-1 receptors correlates with phosphorylation of a single amino acid residue in the forkhead transcription factor FKHR. *EMBO J.* 2000; 19:989–996. [PubMed: 10698940]
- Nakae J, Kitamura T, Silver DL, Accili D. The forkhead transcription factor Foxo1 (Fkhr) confers insulin sensitivity onto glucose-6-phosphatase expression. *J Clin Invest.* 2001; 108:1359–1367. [PubMed: 11696581]
- Negishi H, Ohba Y, Yanai H, Takaoka A, Honma K, Yui K, Matsuyama T, Taniguchi T, Honda K. Negative regulation of Toll-like-receptor signaling by IRF-4. *Proc Natl Acad Sci U S A.* 2005; 102:15989–15994. [PubMed: 16236719]
- Orlicky DJ, DeGregori J, Schaack J. Construction of stable coxsackievirus and adenovirus receptor-expressing 3T3-L1 cells. *J Lipid Res.* 2001; 42:910–915. [PubMed: 11369798]
- Rosen ED, Hsu CH, Wang X, Sakai S, Freeman MW, Gonzalez FJ, Spiegelman BM. C/EBPalpha induces adipogenesis through PPARgamma: a unified pathway. *Genes Dev.* 2002; 16:22–26. [PubMed: 11782441]

- Samad F, Pandey M, Bell PA, Loskutoff DJ. Insulin continues to induce plasminogen activator inhibitor 1 gene expression in insulin-resistant mice and adipocytes. *Mol Med.* 2000; 6:680–692. [PubMed: 11055587]
- Sartipy P, Loskutoff DJ. Expression profiling identifies genes that continue to respond to insulin in adipocytes made insulin-resistant by treatment with tumor necrosis factor- α . *J Biol Chem.* 2003; 278:52298–52306. [PubMed: 14530283]
- Taylor P, Tamura T, Ozato K. IRF family proteins and type I interferon induction in dendritic cells. *Cell Res.* 2006; 16:134–140. [PubMed: 16474425]
- Tamura T, Yanai H, Savitsky D, Taniguchi T. The IRF family transcription factors in immunity and oncogenesis. *Annu Rev Immunol.* 2008; 26:535–584. [PubMed: 18303999]
- Todaro GJ, Green H. Quantitative studies of the growth of mouse embryo cells in culture and their development into established lines. *J Cell Biol.* 1963; 17:299–313. [PubMed: 13985244]
- Uyeda K, Yamashita H, Kawaguchi T. Carbohydrate responsive element-binding protein (ChREBP): a key regulator of glucose metabolism and fat storage. *Biochem Pharmacol.* 2002; 63:2075–2080. [PubMed: 12110366]
- Wang ZV, Deng Y, Wang QA, Sun K, Scherer PE. Identification and characterization of a promoter cassette conferring adipocyte-specific gene expression. *Endocrinology.* 151:2933–2939. [PubMed: 20363877]
- Wiese RJ, Mastick CC, Lazar DF, Saltiel AR. Activation of mitogen-activated protein kinase and phosphatidylinositol 3'-kinase is not sufficient for the hormonal stimulation of glucose uptake, lipogenesis, or glycogen synthesis in 3T3-L1 adipocytes. *J Biol Chem.* 1995; 270:3442–3446. [PubMed: 7852430]
- Wijkander J, Landstrom TR, Manganiello V, Belfrage P, Degerman E. Insulin-induced phosphorylation and activation of phosphodiesterase 3B in rat adipocytes: possible role for protein kinase B but not mitogen-activated protein kinase or p70 S6 kinase. *Endocrinology.* 1998; 139:219–227. [PubMed: 9421418]
- Yang X, Lu X, Lombes M, Rha GB, Chi YI, Guerin TM, Smart EJ, Liu J. The G(0)/G(1) switch gene 2 regulates adipose lipolysis through association with adipose triglyceride lipase. *Cell Metab.* 2010; 11:194–205. [PubMed: 20197052]
- Zheng Y, Chaudhry A, Kas A, deRoos P, Kim JM, Chu TT, Corcoran L, Treuting P, Klein U, Rudensky AY. Regulatory T-cell suppressor program co-opts transcription factor IRF4 to control T(H)2 responses. *Nature.* 2009; 458:351–356. [PubMed: 19182775]
- Zu L, He J, Jiang H, Xu C, Pu S, Xu G. Bacterial endotoxin stimulates adipose lipolysis via toll-like receptor 4 and extracellular signal-regulated kinase pathway. *J Biol Chem.* 2009; 284:5915–5926. [PubMed: 19122198]
- Zuo Y, Qiang L, Farmer SR. Activation of CCAAT/enhancer-binding protein (C/EBP) α expression by C/EBP β during adipogenesis requires a peroxisome proliferator-activated receptor- γ -associated repression of HDAC1 at the C/ebp α gene promoter. *J Biol Chem.* 2006; 281:7960–7967. [PubMed: 16431920]

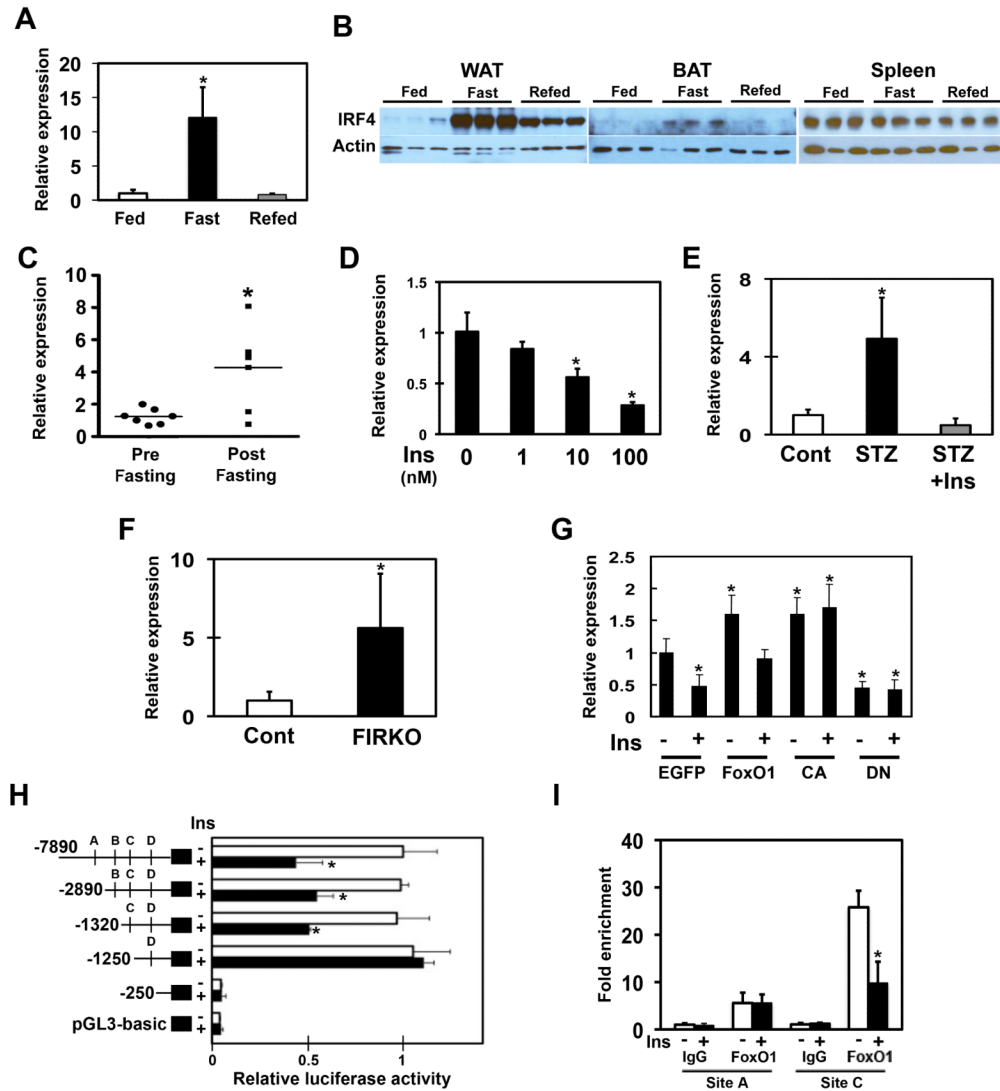


Figure 1. IRF4 expression is regulated during fasting and feeding by insulin and FoxO1
A. Nutritional regulation of *Irf4* mRNA expression in murine white adipose tissue (WAT). Male FVB mice were sacrificed in the fed state, after a 24hr fast, or 24hr after refeeding (n=7-8). Data are normalized to 36B4 expression and are expressed as fold induction relative to *Irf4* mRNA in the fed state. Results expressed as mean \pm SD. **B.** Nutritional regulation of IRF4 protein expression in murine WAT, brown adipose tissue (BAT), and spleen. **C.** *IRF4* mRNA expression in human WAT, sampled pre and post-fasting (n=7). *p<0.05 versus pre fasting. **D.** Regulation of *Irf4* mRNA expression by insulin in 3T3-L1 adipocytes. 3T3-L1 adipocytes were incubated in serum-free DMEM with insulin at the indicated doses for 8hrs (n=3). Data are normalized to 36B4 and presented as expression relative to 0nM insulin. *p<0.05 versus 0nM insulin. Results expressed as mean \pm SD. **E.** *Irf4* mRNA expression in WAT of streptozotocin (STZ)-treated mice. *Irf4* mRNA expression was measured by Q-PCR in WAT of 10-week-old male mice given vehicle (control), STZ, or STZ followed by insulin replacement for 24h (STZ+Ins) (n=8-10/group). Data are normalized to 36B4 and presented as expression relative to control, *p<0.05. Results expressed as mean \pm SD. **F.** *Irf4* mRNA expression in WAT of Fat Insulin Receptor

Knockout (FIRKO) mice (n=4/group). Data are normalized to 36B4 and presented as expression relative to control. Results expressed as mean \pm SD. *p<0.05 versus control. **G.** *Irf4* mRNA expression in 3T3-L1 Δ CAR adipocytes transduced with adenovirus expressing EGFP, wild type (WT), constitutively active (CA), or dominant negative (DN) FoxO1. Data are normalized to 36B4 and presented as fold induction relative to EGFP cells. *p<0.05 versus EGFP cells. Results expressed as mean \pm SD. **H.** Luciferase activity of *Irf4* promoter constructs in 3T3-L1 adipocytes. Five days after adipogenic stimulation, 3T3-L1 cells were transfected with the indicated *Irf4* promoter construct. Luciferase activity was measured 24 hr after transfection in the presence (filled bar) or absence (open bar) of insulin. Results are expressed as mean \pm SD (n = 3). *p < 0.05 relative to the same construct without insulin. Results expressed as mean \pm SD. **I.** ChIP assay of FoxO1 binding to *Irf4* promoter constructs in 3T3-L1 adipocytes in the presence (filled bar) or absence (open bar) of insulin (n=3). All results normalized to IgG without insulin, and expressed as mean \pm SD.

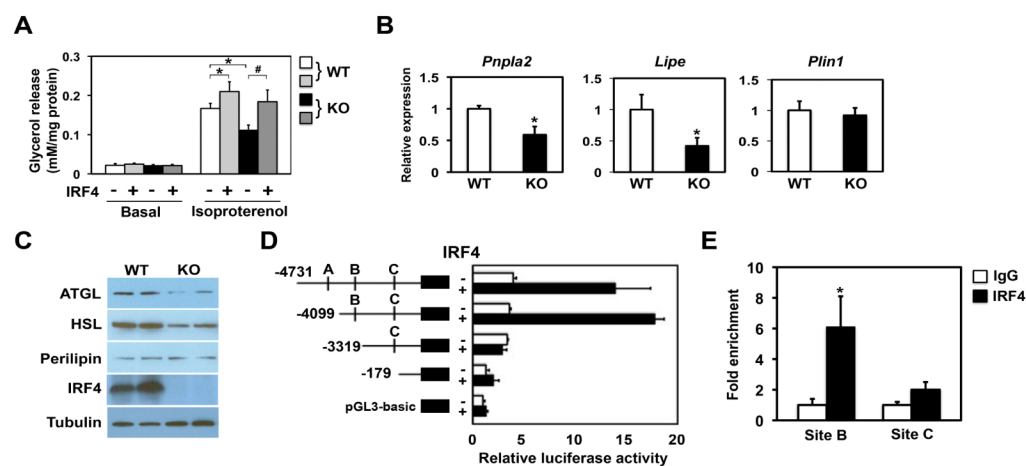


Figure 2. IRF4 promotes lipolysis *in vitro* via effects on lipase expression

A. Basal and isoproterenol-stimulated glycerol release (6-hour stimulation) in WT and KO MEFs, with and without the addition of exogenous IRF4. * $p < 0.05$ ($n = 6$). Results expressed as mean \pm SD. **B.** *Pnpla2*, *Lipe*, and *Plin1* mRNA expression in WT and KO MEFs. * $p < 0.05$ relative to WT control ($n = 3$). Results expressed as mean \pm SD. **C.** ATGL, HSL, and PLIN1 protein expression in WT and KO MEFs. **D.** Luciferase activity of *Pnpla2* promoter reporter constructs transfected into 3T3-L1 adipocytes. Five days after adipogenic stimulation, 3T3-L1 cells were co-transfected with the indicated promoter construct and an IRF4 expression plasmid (or control). Luciferase activity was measured 24 hr after transfection. Results are expressed as mean \pm SD ($n = 6$). * $p < 0.05$ relative to EGFP. **E.** ChIP analysis in 3T3-L1 adipocytes overexpressing IRF4. The signal in IgG is set as 1. Results expressed as mean \pm SD.

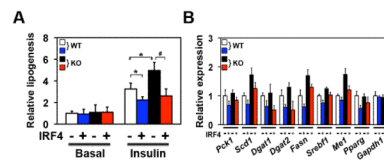


Figure 3. IRF4 inhibits lipogenesis *in vitro*

A. Insulin (100nM) stimulation of ^{14}C glucose incorporation into lipid was determined in WT and KO MEFs, with and without the addition of exogenous IRF4. * $p < 0.05$ ($n = 6$), Results expressed as mean \pm SD, from three independent experiments. * $p < 0.05$ relative to WT control under insulin stimulation, # $p < 0.05$ relative to KO MEF under insulin stimulation. **B.** WT and KO MEFs were transduced with lentivirus expressing IRF4 or EGFP 5 days after differentiation induction. mRNA expression of lipogenesis genes was measured using Q-PCR 7 days after infection. Results expressed as mean \pm SD, $n = 6$.

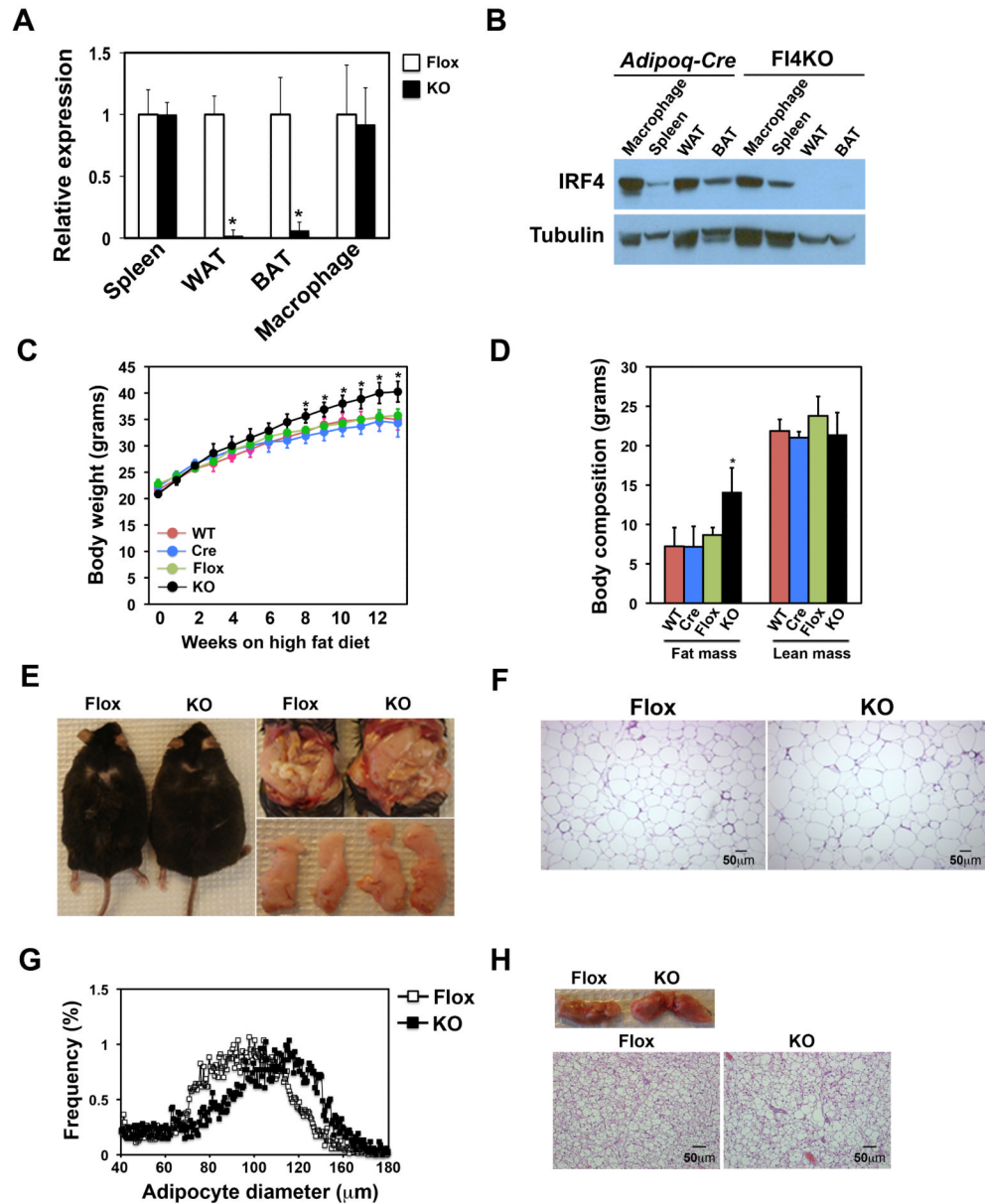


Figure 4. Characterization of Fat-specific IRF4 KO (FI4KO) mice

A. *Irf4* mRNA expression in WAT, BAT, spleen, and peritoneal macrophages of male *Irf4^{fl/fl}* (Flox) and FI4KO (KO) mice (n=3). Data are normalized to 36B4. *p<0.05 relative to Flox mice. Results are expressed as mean ± SD. **B.** IRF4 protein expression in WAT, BAT, spleen, and peritoneal macrophages of male Adipoq-Cre and FI4KO (KO) mice. **C.** Body weights of male WT, Adipoq-Cre, Flox, and FI4KO (KO) mice on high-fat diet (n=8-10). Results are expressed as mean ± SD. **D.** Body composition analysis in 14-week-old male mice (n=8-10) by MRI. Results are expressed as mean ± SD, *p<0.05 relative to Flox mice. **E.** Morphology of FI4KO (KO) mice (16 month old) and fat pads after high-fat feeding. **F.** Hematoxylin and eosin staining of paraffin-embedded epididymal WAT sections from 16-month-old mice. Scale bars = 50µm. **G.** Representative cell size distribution of adipocytes in epididymal WAT from Flox and FI4KO (KO) mice. **H.** Gross appearance and hematoxylin

and eosin staining of paraffin-embedded BAT sections from 16-month-old mice. Scale bars = 50 μ m.

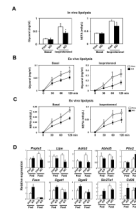


Figure 5. IRF4 is required for lipolysis *in vivo* and *ex vivo*

A. Lipolysis in Flox and FI4KO (KO) mice on chow diet. Glycerol and NEFA in plasma were measured in the absence and presence of 10 μ M of isoproterenol. Results are expressed as mean \pm SD, * p <0.05, versus Flox mice (n=8). **B, C.** Rate of lipolysis in isolated adipocytes. Adipocytes were isolated from epididymal fat of male Flox and FI4KO (KO) mice. Glycerol and NEFA release were measured in the absence and presence of 10 μ M of isoproterenol. Results are expressed as mean \pm SD, * p <0.05 relative to Flox mice (n=3). **D.** Q-PCR analysis of the indicated mRNAs in the adipocyte fraction of epididymal WAT from 12-week-old Flox or FI4KO (KO) mice on chow diet (n=5) under fed and 24h fasting conditions. All samples are normalized to 36B4. Results expressed as mean \pm SD, * p <0.05, versus Flox mice.

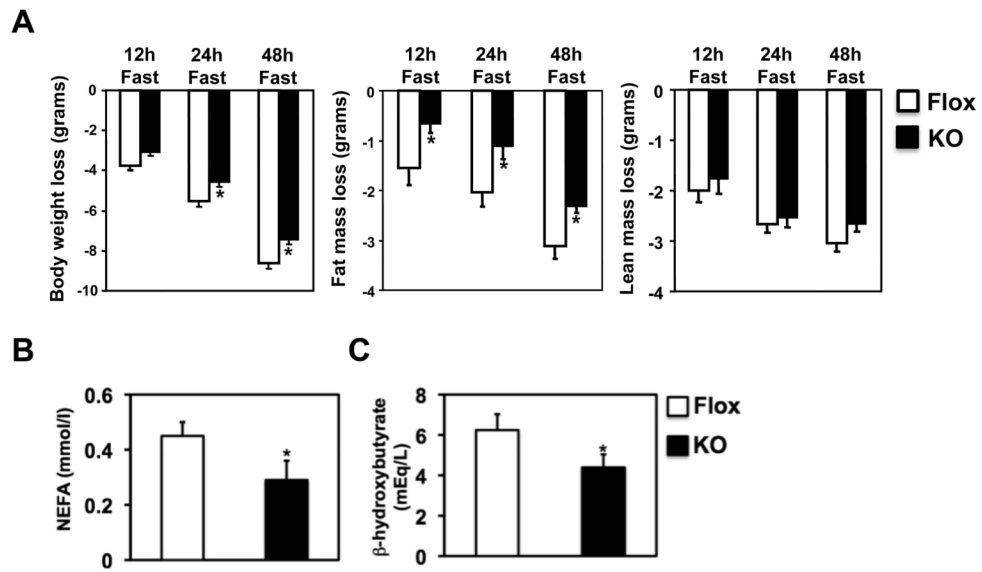


Figure 6. FI4KO mice have an aberrant response to prolonged fasting

A. Response of FI4KO mice to prolonged fasting. Results are expressed as mean \pm SD, * p <0.05 relative to Flox mice ($n=9$). **B.** NEFA levels after 48hr of fasting ($n=9$ mice per group; * p <0.05). **C.** β -hydroxybutyrate levels after 48hr of fasting ($n=9$ mice per group; * p <0.05). Data are expressed as mean \pm SD.

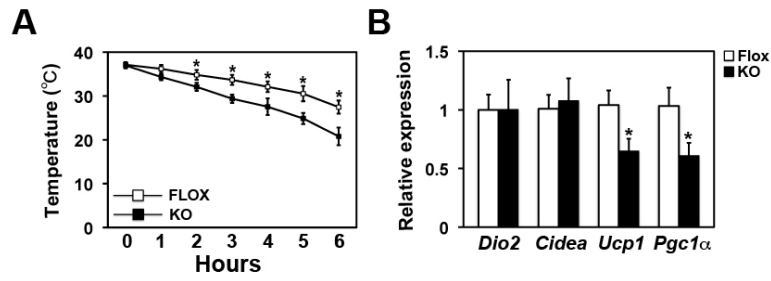


Figure 7. FI4KO mice are cold intolerant

A. Rectal temperature of Flox and FI4KO (KO) mice during cold exposure (4°C). Results are expressed as mean ± SD, * $p < 0.05$ relative to Flox mice (n=7 mice per group). **B.** Expression of *Dio2*, *Cidea*, *Ucp1*, and *Pgc1α* in BAT after cold exposure for 6 hr (n=7 mice per group; * $p < 0.05$). Data are expressed as mean ± SD.